Thermal Performance Analysis of Artificially Roughened Solar Air Heater Using CFD

Shahrukh Khan[1], Prof. Rohit Soni[2]
[1]*Trinity Institute of Technology and Research, Research Scholar, RGPV Bhopal, MP, INDIA*
[2]*Trinity Institute of Technology and Research, Professor, RGPV Bhopal, MP, INDIA*

Abstract- **The twenty-first century is forming into the perfect energy storm. Rising energy prices, diminishing energy availability and security, and growing environmental concerns are quickly changing the global energy panorama. Energy and water are the keys to modern life and provide the basis necessary for sustained economic development. Industrialized societies have become increasingly dependent on fossil fuels for myriad uses. Modern conveniences, mechanized agriculture, and global population growth have only been made possible through the exploitation of inexpensive fossil fuels. Finding sufficient supplies of clean and sustainable energy for the future is the global society's most daunting challenge for the twenty-first century. The future will be a mix of energy technologies with renewable sources such as solar, wind, and biomass playing an increasingly important role in the new global energy economy.**

In the present work attempts are made to performed to study the effects of different rib shapes on heat transfer and fluid flow characteristics through transversely roughened rectangular channels for Reynolds number ranging from 3800 to 15,000 and subjected to uniform heat flux of 1000 W/m2 using CFD. Considering single-phase approach, the three-dimensional continuity, Navier-Stokes, and energy equations developed for the physical model have been solved by using the finite volume method (FVM). The optimization was carried out by using various Rib shapes (X-section rib channel & Square section rib channel) in in-line and different aspect ratios (Dh=33.33, Aspect ratio of duct W/H=5, Relative roughness pitch P/e=7.14, Relative roughness height e/D=0.042) to reach the optimal geometry of the rib with maximum Performance Evaluation Criterion (PEC). The highest PEC was obtained for the X-section rib at Re =3800 is 1.703. For the X-section rib channel, the increase in average Nusselt number value is about 162.48% more than the smooth channel and the use of the X-section rib channel compare with Square section rib channel shows a higher average Nusselt number around 17.70%.

Index Terms- Solar Air Heater, Artificial Roughness, Rib, Absorber Plate, ANSYS 14.5, Reynold's number, Nusselt number, CFD, Fluent

I. INTRODUCTION

1.1 Solar Air Heater

A conventional solar air heating system consists of a blackened absorber plate, glazing/glass cover, supportive walls, ducts or channels for air flow, centrifugal blower or fans to circulate air, and insulation on each side/bottom to reduce conduction losses to environment. Except for the top of SAH, all other sides are well insulated to reduce thermal losses. The convective and radiation losses to the atmosphere are minimized by providing glazing on the top which allows solar radiation to stay between absorber and glazing and to be absorbed by heat-transferring surface. Heat is transferred to fluid flowing through duct underneath the heated plate (Duffie and Beckman 1980).

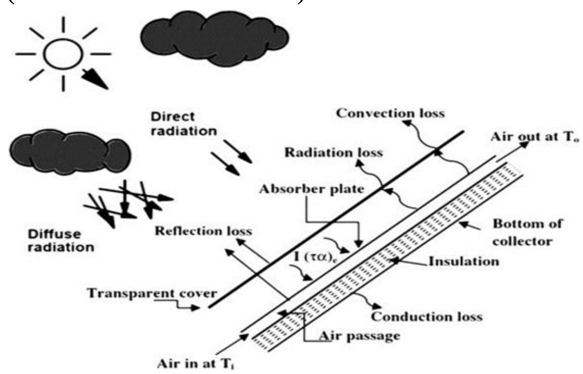

Figure 1: Conventional solar air heater.

SAHs have been used at a wide range for energy saving specially for applications requiring low to moderate air temperatures. They are also used effectively for some applications including space heating, textile, marine products, solar water desalination and crop drying. SAHs have many advantages compared to liquid heaters because of avoiding the problems of freezing or stagnation, leaks, damage and environmental or health hazard risk from the heat transfer medium.

1.2 Classification of Solar Air Heater

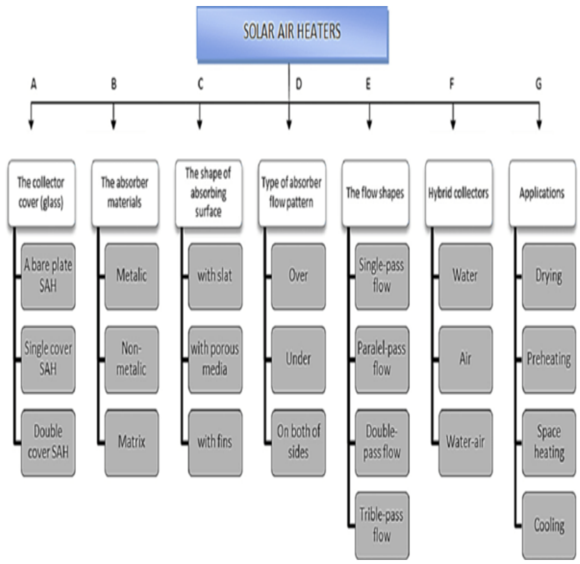

Figure 2: Classification of the SAHs

1.3. Performance representation of SAHs

Performance analysis is essential in order to design an efficient and optimal solar air heating system. Heat-transfer process is a measure of the thermal performance and the pressure drop in the duct tells about the hydraulic performance. The overall performance of the system is represented by the thermo-hydraulic performance and it helps in optimization of geometrical and operational parameters of the system. Performance parameters of a SAH are discussed in the following subsection.

1.3.1. Thermal performance

The thermal performance of a SAH is expressed in terms of its useful heat gain (Qu), specific heat gain (qu), and thermal efficiency (ηth). According to Bliss (1959).

$$q_u = \frac{Q_u}{A_c} = F_R\left[I < \tau\alpha >_e - U_L \frac{(T_{in} - T_a)}{I}\right]$$

$$n_{th} = F_R\left[< \tau\alpha >_e - U_L \frac{(T_{in} - T_a)}{I}\right]$$

1.4 SAH with artificial roughness

Heat-transfer rate from the surface of SAH remains very low, due to the evolution of the laminar sub-layer near the heated wall that provides a resistance to heat flow. Therefore, to enhance the rate of heat transfer from the duct, there is a need to break this layer.

II. LITERATURE REVIEW

A review of the theoretical and experimental investigations carried out for various configurations and geometries on the absorber plate of the SAHs are given below:

Gupta (1993) investigated the effect of relative roughness height, angle of attack and Reynolds number on heat transfer and friction factor in rectangular duct having circular wire ribs on the absorber plate. The maximum enhancement of Nusselt number and friction factor as a result of providing artificial roughness was found to be 1.8 and 2.7 times that of smooth duct.

Karwa, Solanki, and Saini (1999) experimentally investigated the behaviors of a rectangular SAH ducts roughened with chamfered ribs. A chamfer angle of 15°, the heat-transfer rate, and the friction factor were found to be maximum. Compared to using smooth ducts, it was found that the enhancement in the Stanton number was 65–90% while the friction factor was approximately 2.68–2.94 times.

The thermal and hydraulic performance of double flow SAH roughened with multiple C-shaped rib was investigated experimentally by Gabhane and Kanase-Patil (2016). Three rib angles were used for different rib geometries with varying pitch distance, an angle of attack, and Reynolds number. Multiple C-shaped ribs in double flow arrangement provide better heat transfer than other arrangements. Correlations were developed for Nusselt number, friction factor, Stanton number, and thermo-hydraulic performance parameter to increase the usefulness of result.

Alam and Kim (2017) numerically studied the effect of conical protrusion ribs on the thermal performance of the SAH. The parameters investigated in their analysis were relative ribs pitch that varied from 6 to 12 and relative ribs height from 0.020 to 0.044 for the range of Reynolds number from 4,000 to 16,000. The maximum thermal efficiency and efficiency enhancement factor were found to be as 69.8% and 1.346%, respectively.

Kumar et al. (2017) experimentally studied the Nusselt number and friction factor of a SAH duct with multiple V-pattern dimpled type obstacles. On the basis of hydraulic diameter of the duct, the range of Reynolds number (Re) varied from 5,000 to

17,000, relative dimpled obstacles width (W/w) varied from 1to 6, dimpled depth-to-print diameter ratio (e/d) from 0.50 to 2.0, relative dimpled pitch (P/e) varied from 8.0 to 11.0, relative dimpled height (e/D) of values of 0.037, and the angle of attack (α) varied from 35° to 75°. The optimum data of thermal and hydraulic performance obtained at e/D of 0.037, W/w of 5, P/e of 9.0, e/d of 1.0, and α of 55°.
The effect of forward chamfered ribbed absorber plate was studied by Kumar, Goel, and Kumar (2018). Two new roughness parameters named rib aspect ratio (e/w) and rib chamfered height ratio (e0/e) were defined and their influence on the performance of triangular duct SAH was simulated using commercial ANSYS software for Reynolds number (Re) varied between 4,000 and 17,000. The e/w, relative roughness height (e/D), and e0/e range from 0.24 to 1.5, 0.018 to 0.043, and 0 to 1.0, respectively. The enhancements in the peak value of heat transfer and pressure loss were found to be as 2.88 and 3.53 times, respectively, as compared to without ribbed duct.

III.METHODOLOGY

3.1 Model Description and Geometry Setup

A 3-dimensional model the shape of a rectangular duct is developed for solar air heater Analysis .The model geometry is created pre-processor using. The model geometry will be created using pre-processor ANSYS DESIGN MODELER. The physical dimension set to be 640 mm length, 100 mm width, and 20mm height.

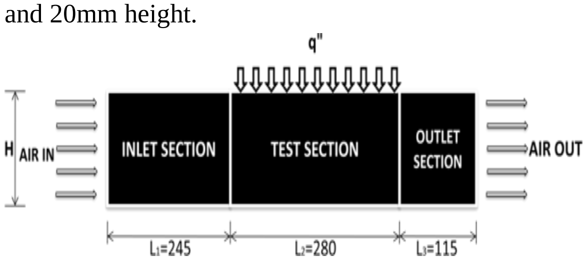

Figure 3: Schematic diagram of the investigated region of smooth rectangular channel.

Table 1 Geometric parameters of Solar air Heater

Operating and Geometrical parameters	Value / Range
Test length of duct, L_2 (mm)	280
Entrance length of duct L_1 (mm)	245
Exit length of duct L_3 (mm)	115
Duct height, H (mm)	20
Duct width, W (mm)	100
Duct hydraulic diameter, Dh (mm)	33.33
Aspect ratio of duct, W/H (mm)	5
Constant heat flux, q" (W/m2)	1000
Reynolds number	3800 - 15000
Rib height e (mm)	1.4
Pitch P (mm)	10
Relative roughness pitch, 'P/e'	7.14
Relative roughness height, 'e/D'	0.042

The assumptions made on the operating conditions of the ribbed channel are as follows:-

1. The ribbed channel operates under steady-state conditions
2. The fluid is incompressible and remains in single-phase along the channel
3. The properties of the fluid and channel material are independent of temperature
4. Uniform heat flux is incident on upper wall

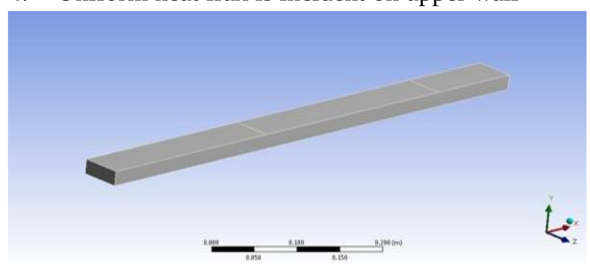

Figure 4 : 3-D domain SAH DUCT of smooth rib

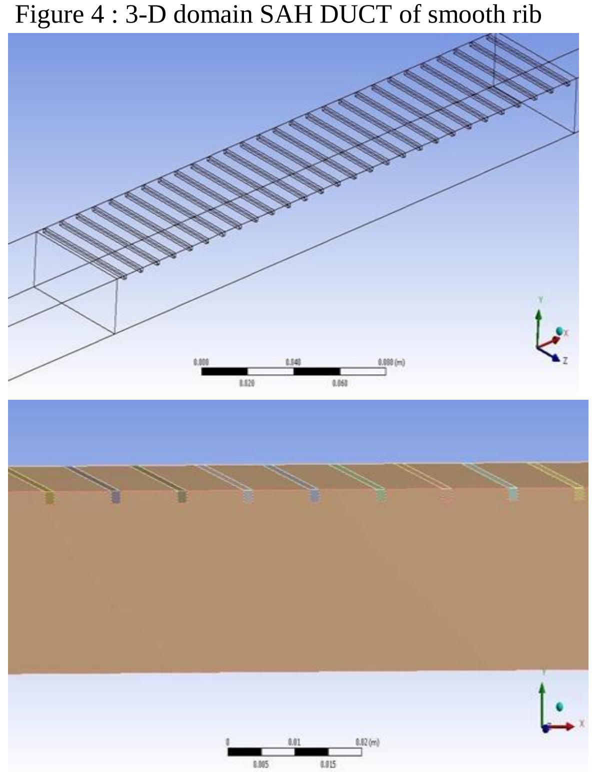

Figure 5: 3-D domain SAH DUCT of square shaped rib

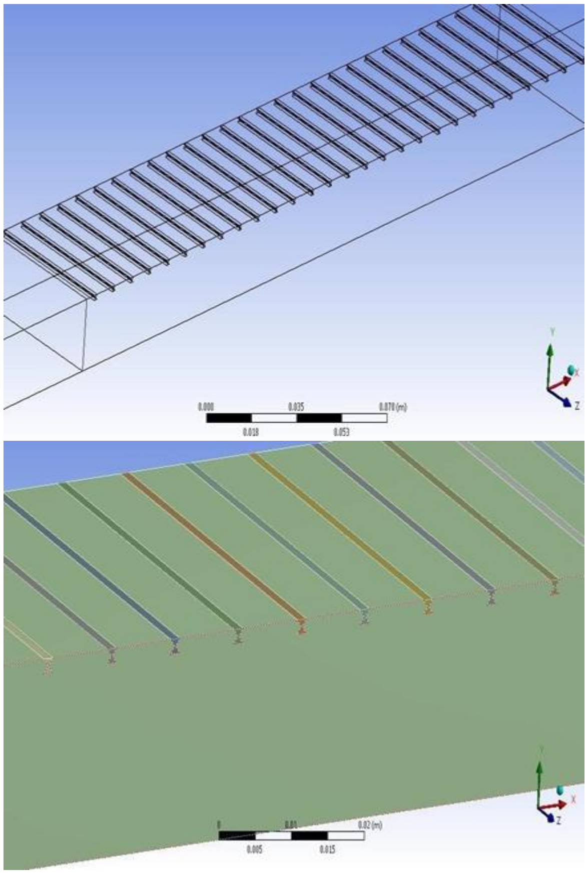

Figure 6: 3-D domain SAH DUCT of X- shaped rib.

3.2 Meshing

By using ANSYS software in meshing edge sizing has been done. Inflation also makes for proper contact mesh.

For Square shaped ribs:

- No. of node: 116843
- No. of element: 310287
- Mesh contains mixed cells per unit area (ICEM Tetrahedral cells) having meshing type tetrahedral and quadrilateral at the boundaries.

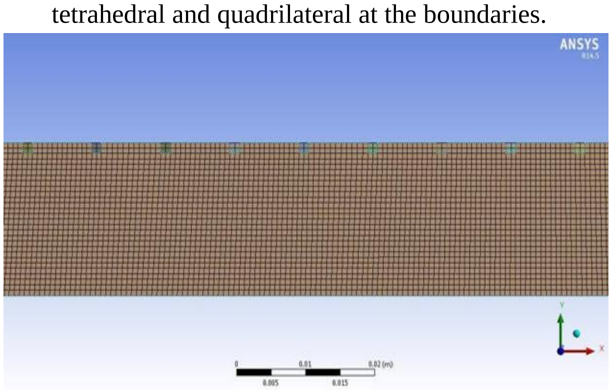

Figure 7: Meshing view 2 for SAH DUCT of square shaped rib

For X- shaped ribs:

- No. of node: 119876
- No. of element: 311343
- Mesh contains mixed cells per unit area (ICEM Tetrahedral cells) having meshing type tetrahedral and quadrilateral at the boundaries.

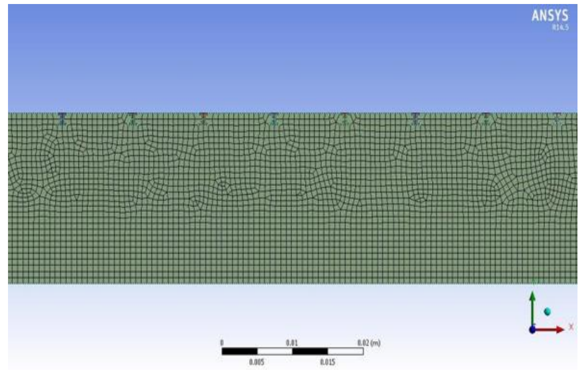

Figure 8: Meshing view 2 for SAH DUCT of X- shaped rib

3.3 Types of Solver

After mesh generation defined the following setup in the ANSYS fluent.

- Problem Type- 3D, Steady State
- Type of Solver- Pressure-based solver

3.4 Model Selection

- Viscous: k- ε (epsilon) two equation turbulence model.
- Pressure- velocity coupling – Scheme -SIMPLE
- Pressure – Standard
- Momentum – Second order
- Energy - second order
- Turbulent Kinetic Energy (k) – second order
- Turbulent Dissipation Rate (e) - second order

3.5 Material Selection

Table 2 Material selection for Solar air Heater

Properties	Air	Absorber plate (Aluminium)
Density, ‘ρ’ (Kg/ m3)	1.225	2719
Specific heat, ‘c_p’ (J-Kg/K)	1006.43	871
Thermal conductivity, ‘k’(W/ m-K)	0.0242	202.4
Viscosity, ‘μ’ (N-s/m2)	1.79×10-5	---
Prandtl number	0.71	---

3.6 Boundary Conditions

- Operating Condition- Pressure = 101325 Pa

- Inlet- Reynolds number in the range between 3800 and 15000.

Ambient temperature of Tin = 300 K
Turbulent intensity = 1%
Hydraulic Dia. = 33.33 mm
Heat flux at the top of the absorber plate, q = 1000W/m2
*The mean inlet velocity of the flow is calculated using Reynolds number.

- Outlet- Pressure outlet: Define the same outlet condition for all the fan outlet

Gauge pressure = 0 Pa
For viewing and interpretation of Result. The result can be viewed in various formats, graph, value, animation etc.

IV. RESULTS AND DISCUSSIONS

The data collected using ANSYS FLUENT 14.5 included the temperature distribution, pressure distribution and airflow velocity at all node points in the model duct. We can see the following result-

Contours for SAH DUCT of X-shaped rib

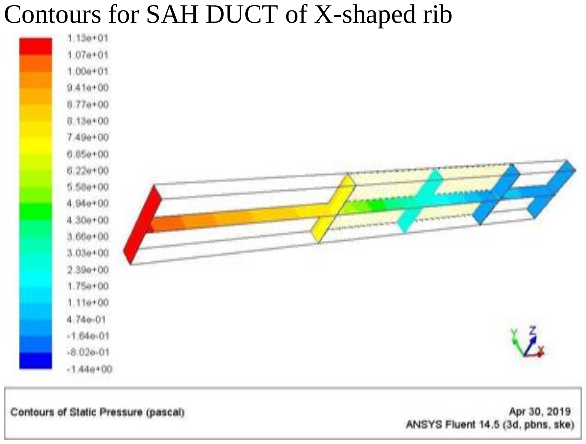

Figure 9 Pressure Contour of X- Rib Section channel

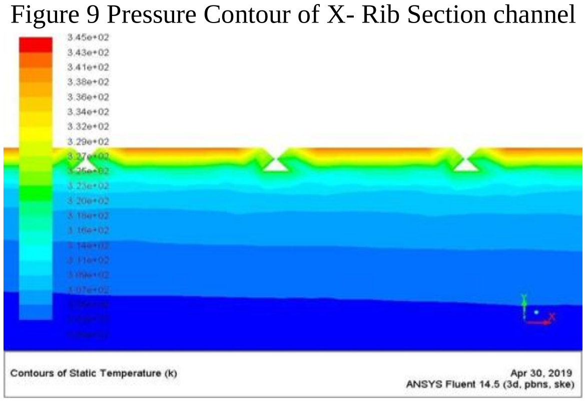

Figure 10 Temperature Contour 1 of X- Rib Section channel

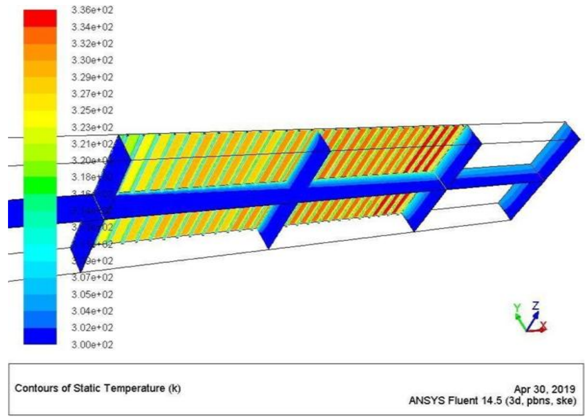

Figure 11 Temperature Contour 2 of X- Rib Section channel.

4.4 Performance Evaluation

The Nusselt number ratio, Nurib⁄Nus, defined as a ratio of average Nusselt number of rib channel to average Nusselt number of smooth channel and the value of ratio plotted against the Reynolds number value, is shown in Fig. 12 In this figure, the Nusselt number ratio tends to decrease with the rise of Reynolds number From 3,800 to 15,000 for all ribs shows a slightly increase for higher Reynolds number value. The average Nurib⁄Nus, values for the X-section rib & Square section rib are respectively, around, 2.717, and 2.401 at Re no. 3800.

Figure 12 Variation of Nusselt number ratio, Nu(rib)/Nu(smooth) with Reynolds number

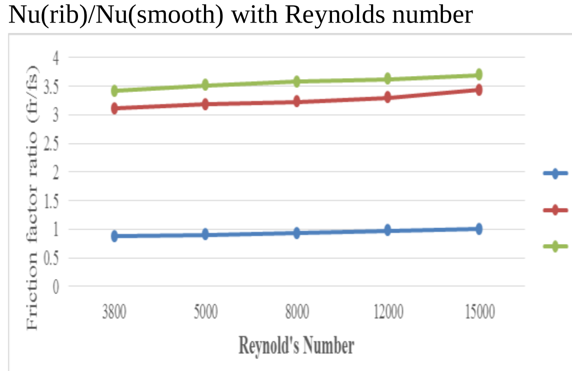

Figure 13 Variation of friction factor ratio, f(rib)/f(smooth) with Reynolds number

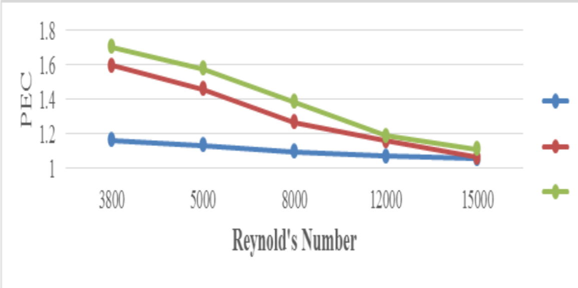

Figure 14 PEC with Reynolds number.

V. CONCLUSIONS

A 3-dimensional CFD analysis has been carried out to study heat transfer and fluid flow behavior in a rectangular duct of a solar air heater with one roughened wall having square and x-shaped rib roughness. The effect of Reynolds number on the heat transfer coefficient and friction factor have been studied. In order to validate the present numerical model, results have been compared with available experimental results under similar flow conditions. CFD Investigation has been carried out in medium Reynolds number flow (Re 3800-15, 000). The following conclusions are drawn from present analysis:

- X-section rib channel shows the maximum average Nusselt number as compared to other rib shape channel for all value of Re from 3800 to 15,000, and its value is approximately 2.717 times more of smooth channel at Re=3,800.
- X-section rib channel shows the maximum average friction factor as compared to other rib shape channel for Re vary from 3800 to 15,000, and its value 3.7 times more of smooth channel.
- In X-section rib channel shows maximum value of Performance Evaluation Criteria (PEC) is 1.703, Square section rib channel of PEC is 1.596, all the value is found at Reynolds number Re=3,800.

REFERENCES

[1] Duffie, J. A., and W. A. Beckman. 1980. Solar engineering of thermal processes. New York: Wiley.
[2] Gupta D, Solanki SC, Saini JS. Heat and fluid flow in rectangular solar air heater ducts having transverse rib roughness on absorber plates. Solar Energy 1993;51(1):31–7.
[3] Garg, H. P., and J. Prakash. 1997. Solar energy fundamentals and applications. New Delhi: Tata Mc Graw-Hill.
[4] Ekechukwu OV, Norton B. Review of solar-energy drying systems II: an overview of solar drying technology. Energy Convers Manag 1999;40(6):615–55.
[5] Karwa, R., S. C. Solanki, and J. S. Saini. 1999. Heat transfer coefficient and friction factor correlations for the transitional flow regime in rib-roughened rectangular ducts. International Journal of Heat and Mass Transfer 42:1597–615.
[6] Mathur, A. N., and Y. C. Bhatt. 2002. Solar based energy sources in the millennium 2000. Paper presented at the All India Seminar on Advances on Solar Energy Technologies, Jodhpur, Rajasthan, India: Department. Of Mechanical Engineering, M.B.M. Engineering College, Jai Narayan Vyas University.
[7] Jaurker, A. R., J. S. Saini, and B. K. Gandhi. 2006. Heat transfer and friction characteristics of rectangular solar air heater duct using rib-grooved artificial roughness. Solar Energy 80:895–907.
[8] Jain Amit, Bhagoria JL, Sharma MC. Thermal performance of solar air heater by using shot peened absorber plate, 46. Bhopal (M.P)-India: Mechanical Engineering Department, MANIT; 2007. p. 667–73.
[9] Hwang, S. D., H. G. Kwon, and H. H. Cho. 2008. Heat transfer with dimple/ protrusion arrays in a rectangular duct with a low Reynolds number range. International Journal of Heat and Fluid Flow 29:916–26.
[10] Lanjewar, A., J. L. Bhagoria, and R. M. Sarviya. 2011. Heat transfer and friction in solar air heater duct with W-shaped rib roughness on absorber plate. Energy 36:4531–41.
[11] Tyagia VV, Panwarb NL, Rahima NA, Kotharic Richa. Review on solar air heating system with and without thermal energy storage system. Renew Sustain Energy Rev 2012;16:2289–303.
[12] Sethi, M., and N. S. Thakur. 2012. Correlations for solar air heater duct with dimpled shape roughness elements on absorber plate. Solar Energy 86:2852–61.

[13] Kumar, A., R. P. Saini, and J. S. Saini. 2013. Development of correlations for Nusselt number and friction factor for solar air heater with roughened duct having multi v shaped rib with gap rib as artificial roughness. Renewable Energy 58:151–63.